Inflammation Research (2019) 68:751–760
https://doi.org/10.1007/s00011-019-01258-4

Inflammation Research

ORIGINAL RESEARCH PAPER

Inhibition of JAK2/STAT3 signaling pathway protects mice from the DDP-induced acute kidney injury in lung cancer

Lei Zhang[1] · Peng Lu[1] · Xu Guo[2] · Ting Liu[2] · Xu Luo[3] · Yi-Tang Zhu[1]

Received: 17 March 2019 / Revised: 20 May 2019 / Accepted: 5 June 2019 / Published online: 26 June 2019

Abstract

Objective To explore AG490 (the inhibitor of Janus kinase (JAK) 2/signal transducer and activator of transcription (STAT) 3 pathway) in cisplatin (DDP)-induced acute kidney injury (AKI) in mice with lung cancer.

Methods Mice were randomly divided into normal, model, AG490, DDP and DDP + AG490 groups. The lung cancer models were established except for Normal group. The levels of blood urea nitrogen (BUN) and creatinine and the status of oxidative stress were detected. Then, histological changes were assessed by HE and PAS staining and apoptosis by TUNEL experiment. The molecule expressions were detected by qRT-PCR and western blot, and immunohistochemistry, respectively.

Results DDP inhibited the tumor growth in mice with lung cancer, which was further promoted by the combination with AG490. Mice in the DDP group had elevated levels of BUN and creatinine than those in the Normal group with the increased inflammatory cytokines (TNF-α, IL-6, MCP-1 and CXCL-1) and malondialdehyde (MDA) level and the decreased glutathione (GSH), superoxide dismutase (SOD) and catalase (CAT). In addition, DDP could activate the JAK2/STAT3 pathway to promote the apoptosis by upregulating Bax, cleaved caspase-9 and cleaved caspase-3 while downregulating the Bcl-2 in the kidney tissues. DDP + AG490 group showed the alleviated AKI and the improvements in oxidative stress, inflammatory responses and apoptosis in the kidney tissues, as compared to DDP group.

Conclusion AG490 alleviated DDP-induced AKI in lung cancer mice with improved oxidative stress and inflammation, and the suppression of JAK2/STAT3 pathway.

Keywords Lung cancer · JAK2/STAT3 · Cisplatin · Acute kidney injury

Background

Lung cancer is recognized as the primary factor leading to cancer-related death worldwide, with an increasing trend in both prevalence and mortality [1]. Basically, it consists of approximately 15% of small-cell lung cancer (SCLC) and 85% of non-small-cell lung cancer (NSCLC) [2]. In usual, patients with early diagnosis and timely surgical resection may have a better prognosis with a 5-year survival rate of 70% [3], but most of patients have progressed into advanced stage when diagnosed, which, consequently, contributes to the low survival rate, regardless of major progress in lung cancer treatment in recent years [4]. Cisplatin (DDP) is a kind of drug developed for chemotherapy and widely used as the first-line treatment of lung cancer [5]. DDP is the complex of the Pt^{2+} binding to two chlorine atoms and two molecules of ammonia, exerting the obvious inhibitory influence on the DNA replication [6]. Meanwhile, it has been reported that DDP could also trigger the various adverse reactions, including kidney toxicity, attracting great attention in clinic [7–9]. Thus, rationale use of DDP to minimize the kidney toxicity has become a top issue to be resolved currently.

Janus kinase (JAK)/signal transducer and activator of transcription (STAT) signaling pathway is believed as a key link implicated in cell growth and apoptosis, and also

Responsible Editor: John Di Battista.

Lei Zhang and Peng Lu have equal contribution.

✉ Yi-Tang Zhu
zhu_yitang9@126.com

[1] Department of Clinical Laboratory, Cangzhou Central Hospital, No. 16, Xinhua Western Road, Cangzhou 3061001, Hebei, China

[2] Department of Clinical Laboratory, the 252nd Hospital of PLA, Baoding, China

[3] Department of Pharmacy, Cangzhou Central Hospital, Cangzhou, China

modulates immune and inflammatory responses in humans [10, 11]. Activated JAK could phosphorylate the tyrosine of STAT, and the phosphorylated STAT is able to be transferred into the nucleus to bind to the specific promotor to induce the expression of target mRNAs [12]. STATs are a group of DNA-binding proteins consisting of six members, like STAT1, STAT2, STAT3, STAT4, STAT5 and STAT6 [13, 14]. Among them, STAT3, as a newly discovered oncogene in many literatures, has been pointed out to have a close relationship with the tumors, which was continuously activated in the development and progression of malignancies [15, 16]. On the contrary, blocking the JAK2/STAT3 signaling pathway can improve the sensitivity of tumor cells against DDP, including cervical cancer, esophageal cancer, and lung cancer [17–19]. Furthermore, increasing studies have uncovered the mitigated kidney injuries owing to the inhibition of JAK2/STAT3 pathway. For example, the work of Zhu et al. reported that suppression of the JAK2/STAT3 pathway ameliorated acute kidney injury (AKI) in rats with acute pancreatitis [20], which could be also functioned as a potential target in early intervention of the acute ischemic kidney failure in the study of Yang et al. [21]. Naturally, we inferred that JAK2/STAT3 pathway inhibition may suppress the growth of lung tumors and alleviate the DDP-induced kidney injury in lung cancer mice. Thereafter, in this work, we established the mice models of lung cancer, and further developed AKI models by DDP injection, or intervened by injection of AG490 (the JAK2/STAT3 pathway inhibitor), to observe the potential use of AG490 on the tumor growth and the kidney injury in lung cancer mice.

Materials and methods

Subjects

A total of 50 C57/BL6 mice (8-week-old, half male and half female) were purchased from the Beijing Vital River Laboratory Animal Technology Co., Ltd, who were all kept at 22–25 °C and in circadian rhythm, and had the free access to the food and water in a clean room. Animal-related experiment protocols had been approved by the Ethic Committee for the Experimental Animals in Cangzhou Central Hospital, and all behaviors relating to the experimental animals were conducted under the regulations of animal protection and use of the International Association for the Study of Pain (IASP) [22].

Model establishment and mice grouping

Mice were randomly divided into five groups: Normal group, Model group, DDP group, AG490 group and AG490 + DDP group, with 10 mice (half male and half female) in each group. Except for the mice in the Normal group, those in other four groups were used to establish the lung cancer models using the murine Lewis lung cancer cells. In brief, cell suspension at density of 2×10^6/mL was prepared using the Lewis lung cancer cells and then inoculated subcutaneously at the axilla of the right forelimb. For each mouse, 0.2 mL cell suspension was given, followed by daily regular feeding and observation of the tumor growth. Four days later, tumors were touchable, and the major diameter was about 0.8 ± 0.1 cm. Then, drugs were given intratumorally according to the grouping standards: Model group (intraperitoneal injection (i.p.) of normal saline); DDP group (mice received 10.0 mg/kg DDP, i.p.); AG490 group (mice received 0.5 mg/kg AG490, i.p.); AG490 + DDP group, sequential administration of AG490 (0.5 mg/kg, i.p.) and DDP (10.0 mg/kg, i.p.).

Specimen collection

Fourteen days following the drug administration, the body weight of mice was recorded. Then, mice were anesthetized for collection of serum samples to measure the blood urea nitrogen (BUN) and creatinine. Kidney was dissected thoroughly and was cut into pieces for three parts after weighing for the detection of molecule expressions by qRT-PCR and Western blot, the measurement of oxidative stress indexes, and the kidney histological changes by hematoxylin and eosin (HE) staining and periodic acid-Schiff (PAS) staining. Solid tumors were also dissected, and the tumor volume was calculated by the formula: tumor volume (length $\times$ width^2)/2. The inhibitory rates of the weight (IW) and volume (IV) of tumor were calculated according to the following formulas [23]: IW = (1 − the weight of tumor of experimental group/the weight of tumor of model group) × 100%; IV = (1 − the volume of tumor of experimental group/the volume of tumor of model group) × 100%.

Histological analysis

HE staining: kidney tissues ($n = 10$ in each group) were used to prepare the pathologic sections in thickness of 5 μm following the fixation, clearing, dehydration, waxing and paraffin-embedding. The sections were randomly selected for regular dewaxing in xylene and hydration in the ethanol in gradient concentrations. Thereafter, nucleus was stained using the hematoxylin, and blued in running water, while the cytoplasm was stained using the eosin. Following the staining, sections were subjected to the dehydration, clearing and mounting using the neutral balsam, and placed under the optic microscope to observe the changes in the kidney tissues. PAS staining: The sections ($n = 10$ in each group) in thickness of 5 μm were randomly selected to dewax and hydrate, and then stained in PAS dye. Following the staining, sections were dehydrated, cleared and mounted in neutral balsam, and then placed under the optic microscope to detect the changes in kidney tissues.

qRT-PCR

TRIzol (Invitrogen Inc., Carlsbad, CA, USA) was used to extract the RNA from the tissues ($n=10$ in each group), which was subjected to the measurement of concentration and preserved at − 80 °C for later use. Primers were designed according to the gene sequences in the Genbank using the Primer 5.0 software, and synthesized by GenePharma Co., Ltd. (Shanghai, China). Reaction system was prepared according to the instructions of the One Step SYBR® and PrimeScript® PLUS RT- PCR Kit (Takara). With β-actin as the internal reference, the relative expression was calculated by $2^{-\Delta\Delta Ct}$.

Western blot

Tissues ($n=10$ in each group) were homogenized in presence of lysis buffer, and the total proteins were extracted by centrifugation. Protein concentrations were determined using the BCA kit, and accordingly, 30 µg of proteins were loaded for sodium dodecyl sulfate polyacrylamide gel electrophoresis (SDS-PAGE), and then transferred on the polyvinylidene fluoride (PVDF) membrane. Membrane was then immersed in the 5% skimmed milk/Tris-buffer saline (TBS) for blocking for 1 h at room temperature. Membrane was then washed in TBS (5 min × 3 times), and proteins on the membrane were probed using the primary antibodies at 4 °C overnight. Following 3 washes in TBS (5 min per wash), the immunoblots were incubated with the secondary antibodies at room temperature for 1 h. After 3 washes in TBS (10 min per wash), membrane was subjected to the band development using the enhance chemiluminescence (ECL) reagent, and the bands were analyzed in the gel imaging analyzer.

Detection of oxidative stress indicators

The oxidative stress indicators were detected according to the corresponding methods ($n=10$ for each group). In brief, thiobarbituric acid reactive substance (TBARS) method was employed to determine the content of malondialdehyde (MDA). GSH could interact with the 5,5′-dithiobis nitrobenzoic acid (DTNB) to trigger the color reactions, and the GSH content could be reflected by the optical density of product at wavelength of 412 nm. Catalase activity was determined by the reaction between the enzyme, methanol and H_2O_2 in an optimal concentration, while SOD activity was reflected by the method of Elstner and Heupel [24].

TUNEL staining

Immunofluorescence for TUNEL staining was performed with fluorescein isothiocyanate (FITC). Paraffin sections ($n=10$ in each group) were dewaxed and hydrated sufficiently. Then, they were immersed in the 3% H_2O_2–methanol for 10–15 min, and incubated with protease K at room temperature for 15–30 min. After washes in PBS, sections were treated with TUNEL mixture (50 µL) for 60 min at 37 °C, and washed in PBS for 3 times. Then the sections were mounted with Vectashield mounting medium containing 40,6-diamidino-2-phenylindole (DAPI, Vector Laboratories, Burlingame, CA, USA) for nuclear staining and imaged under a fluorescent microscope (Leica, Wetzlar, Germany). Cells in 10 random high-power fields stained green fluorescence and DAPI stained blue fluorescence were detected as TUNEL-positive apoptotic cells.

Immunohistochemistry (IHC) staining

Sections ($n=10$ in each group) were dewaxed and hydrated regularly, and washed in PBS for three times. Then, they were incubated in presence of 3% H_2O_2 for 10 min at room temperature, which was removed by three washes in PBS (5 min per wash). On the sections, the normal goat serum or 1% bovine serum albumin was dropped for blocking for 30 min at room temperature. Primary antibodies (anti-caspase-3 and anti-CD45) were dropped on the sections for incubation at 4 °C overnight, and after being placed at the room temperature for 30 min, the residual antibodies were removed by 3 washes in PBS (5 min per wash). Sections were then incubated with the secondary antibodies at room temperature for 30 min, followed by washes in PBS, and then incubated in DAB. Color reactions were terminated in the running water. Sections were re-dyed in hematoxylin for 1 min. Differentiation was performed in 1% hydrochloric acid and alcohol. Sections were rinsed in running water for 1 min, dehydrated in ethanol in gradient concentrations and cleared in xylene, and mounted using the neutral balsam. Sections were placed under the optic microscope for photographing.

Statistical analysis

SPSS 21.0 statistical software was adopted for data analysis. All experiments were repeated for three times or more to calculate the means and standard deviation. Measurement data were expressed in form of mean ± standard deviation. Comparisons among groups were performed using the One-way analysis of variance (One-way ANOVA), and intergroup comparison using the Tukey's test. $P < 0.05$ represented the significant difference.

Results

AG490 enhanced the inhibitory effect of DDP on the tumor growth in lung cancer mice

As shown in Fig. 1, the tumor volume and tumor mass were in a declined trend in mice from AG490 group, DDP group and DDP + AG490 group when compared to those from Model group (all $P < 0.05$). Besides, the weight and volume inhibitory rates (IW and IV) of mice from DDP group, AG490 group and DDP + AG490 group were (38.97% and 43.51%), (12.26% and 16.83%) and (72.17% and 67.79%), respectively. These results suggested that both AG490 and DDP could inhibit the tumor growth in lung cancer mice, and AG490 could further enhance the inhibitory effect of DDP on tumor growth.

Protection of AG490 on DDP-induced nephrotoxicity in mice with lung cancer

Mice in the Model group and AG490 group had no significant differences with respect to kidney weight, BUN and SCr when compared to Normal group (all $P > 0.05$), while the decrease in kidney weight were found in mice from DDP group and DDP + AG490 group with the increase in BUN and SCr levels (all $P < 0.05$, Fig. 2). In addition, mice in the DDP + AG490 group had higher kidney weight and lower levels of BUN and SCr than those in the DDP group (all $P < 0.05$).

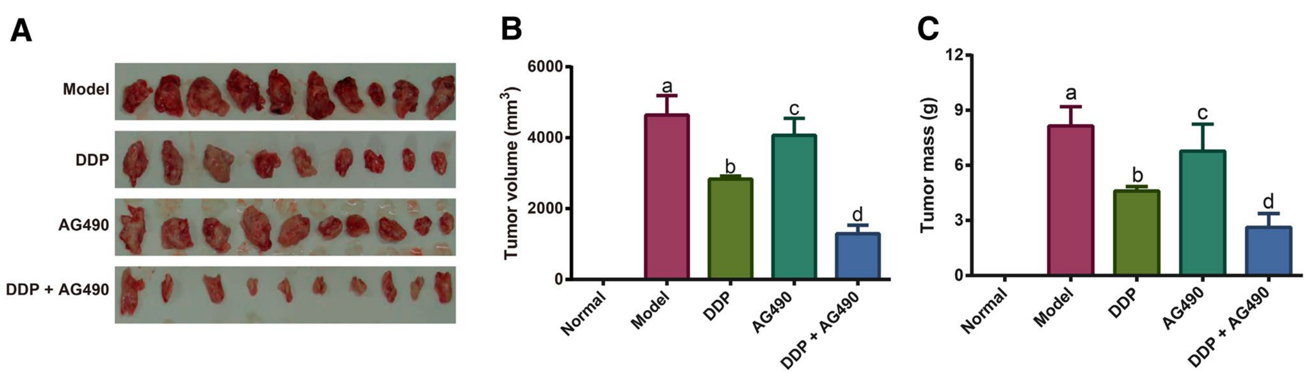

Fig. 1 The growth of implanted Lewis lung cancer in mice ($n = 10$). **a** Implanted tumors after peeled off in each group; **b**, **c** comparison of the tumor volume (**b**) and tumor mass (**c**) among groups. The same letter shows no statistical significance, i.e., $P > 0.05$, while the different letter demonstrates the significant difference, i.e., $P < 0.05$

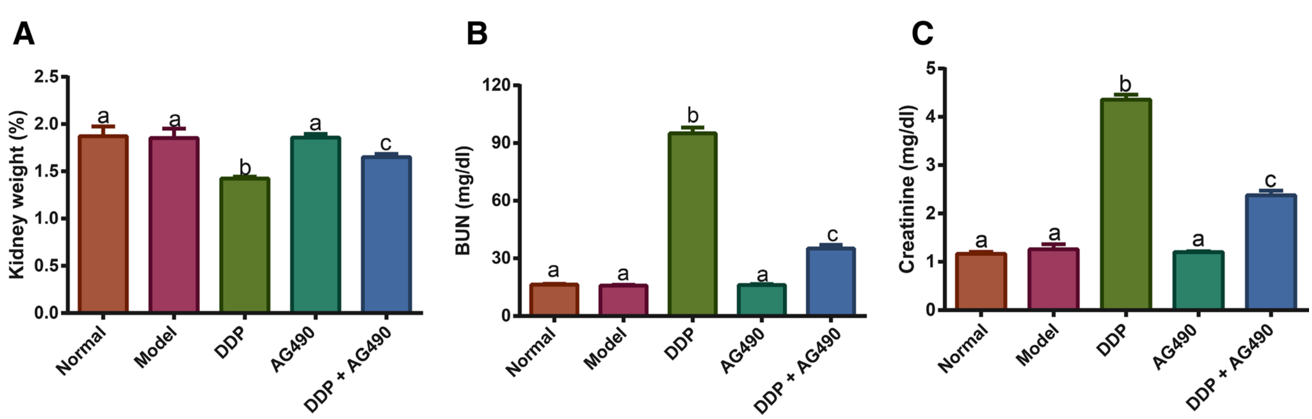

Fig. 2 Effect of AG490 on DDP-induced changes in the kidney weight (**a**), BUN (**b**) and SCr **c** in lung cancer mice ($n = 10$). Kidney weight expressed as the percentage of the total body weight. The same letter shows no statistical significance, i.e., $P > 0.05$, while the different letter demonstrates the significant difference, i.e., $P < 0.05$

Kidney histological changes in different groups

In the normal group, model group and AG490 group, kidney glomeruli and the surrounding kidney tubules were in normal structure with little glycogen sedimented, while the extracellular matrix was in normal distribution. As for DDP group, the basic pathobiology changes were glomeruli enlargement, tubular lumen dilatation, tubular epithelial cell necrosis, inflammatory cell infiltration, and glomerular basement membrane thickening, with massive glycogen sedimentation. Besides, to determine the inflammation status, we performed CD45 immunohistochemistry analysis, and we found the CD45 staining was significant increase in kidney tissues of mice from DDP group as compared with Model group and AG490 group. However, these changes were clearly ameliorated in the DDP + AG490 group (Fig. 3).

Expression of JAK2/STAT3 signaling pathway in different groups

As performed by qRT-PCR in Fig. 4a, the mRNA expressions of *JAK2* and *STAT3* could be upregulated by DDP, but were reduced in presence of AG490 (all $P<0.05$). Meanwhile, no statistical significance was observed between Normal group and DDP + AG490 group concerning *JAK2* and *STAT3* mRNA levels (all $P>0.05$). Western blot analysis also indicated that DDP could activate the JAK2/STAT3 signaling pathway, with up-regulations of p-JAK2 and p-STAT3 (all $P<0.05$), and this effect could be also reversed by AG490 (Fig. 4b, c).

Inhibitory effect of AG490 on DDP-induced inflammation and oxidative stress in lung cancer mice

When compared to the Model group, the levels of TNF-α, IL-6, MCP-1 and CXCL1 were increased in the DDP group and DDP + AG490 group, while AG490 could decrease these inflammation cytokines, as analyzed by qRT-PCR (all $P<0.05$, Fig. 5). No differences of these cytokines were discovered among the Normal group, Model group and AG490 group (all $P>0.05$). Besides, mice in the DDP group and DDP + AG490 group had an increase in MDA with the reduction in GSH, SOD and CAT, as compared to the Model group (all $P<0.05$), but no significant difference was identified between Normal group and AG490 group (all $P>0.05$). Thus, DDP-induced oxidative stress were then ameliorated after administration of AG490, concomitant with the decrease in MDA, but increases in GSH and activities of SOD and CAT (Fig. 6).

Inhibitory effect of AG490 on DDP-induced kidney apoptosis in lung cancer mice

TUNEL results (Fig. 7a) showed no statistical significance in kidney apoptosis among the Normal group, Model group and AG490 group (all $P>0.05$). At the same time, mice in the DDP group had an elevated kidney apoptosis in comparisons with these groups, but the kidney apoptosis in mice from the DDP + AG490 group was reduced (all $P<0.05$). In addition, the apoptotic factors (including Bcl-2, Bax, cleaved caspase-9 and cleaved caspase-3) examined by

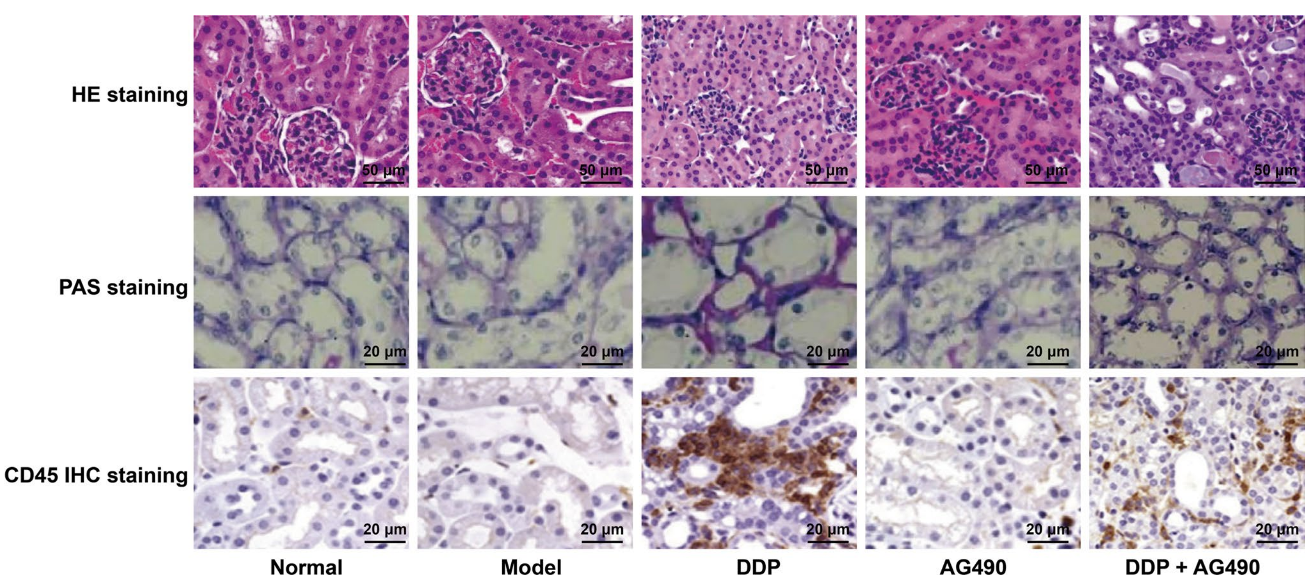

Fig. 3 Effect of AG490 on kidney histological changes in DDP-induced AKI in mice with lung cancer ($n=10$). *HE* hematoxylin–eosin, *PAS* periodic acid-Schiff, *IHC* immunohistochemistry

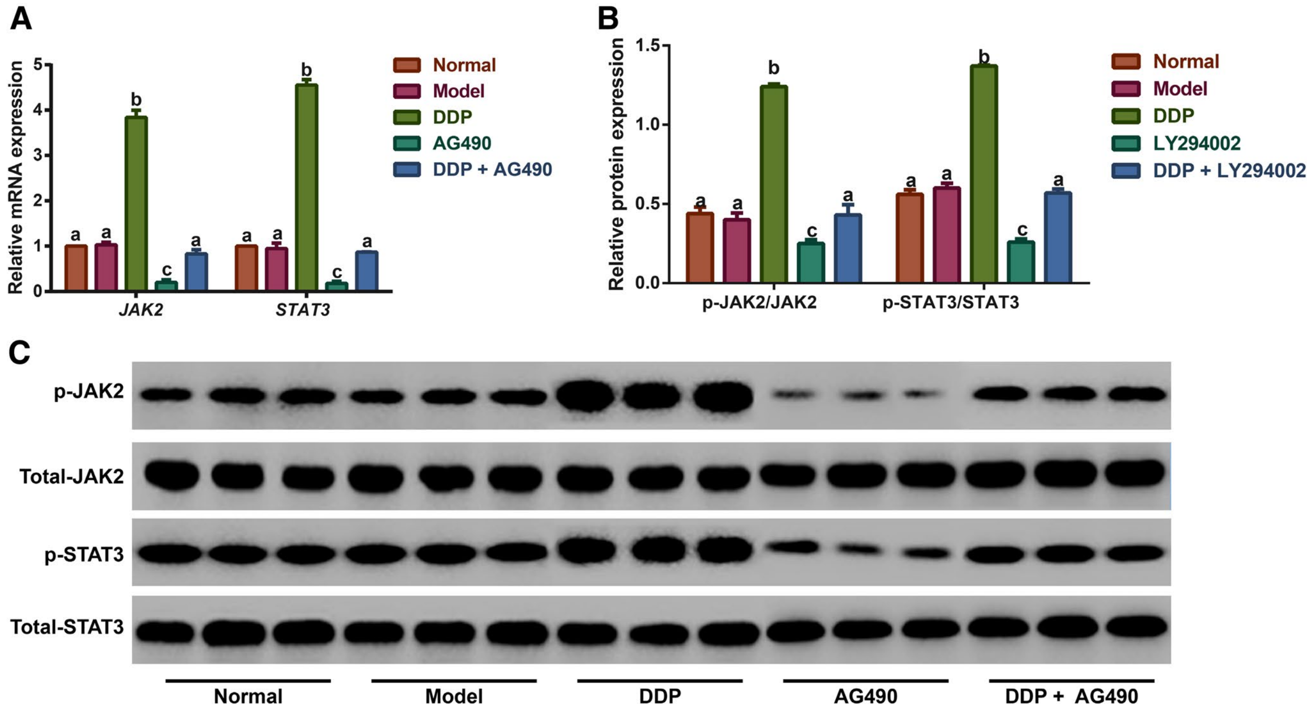

Fig. 4 Expressions of JAK2/STAT3 signaling pathway in kidney tissues of mice in different groups by qRT-PCR (**a**) and Western blot (**b**, **c**) ($n=10$). The same letter shows no statistical significance, i.e., $P>0.05$, while the different letter demonstrates the significant difference, i.e., $P<0.05$

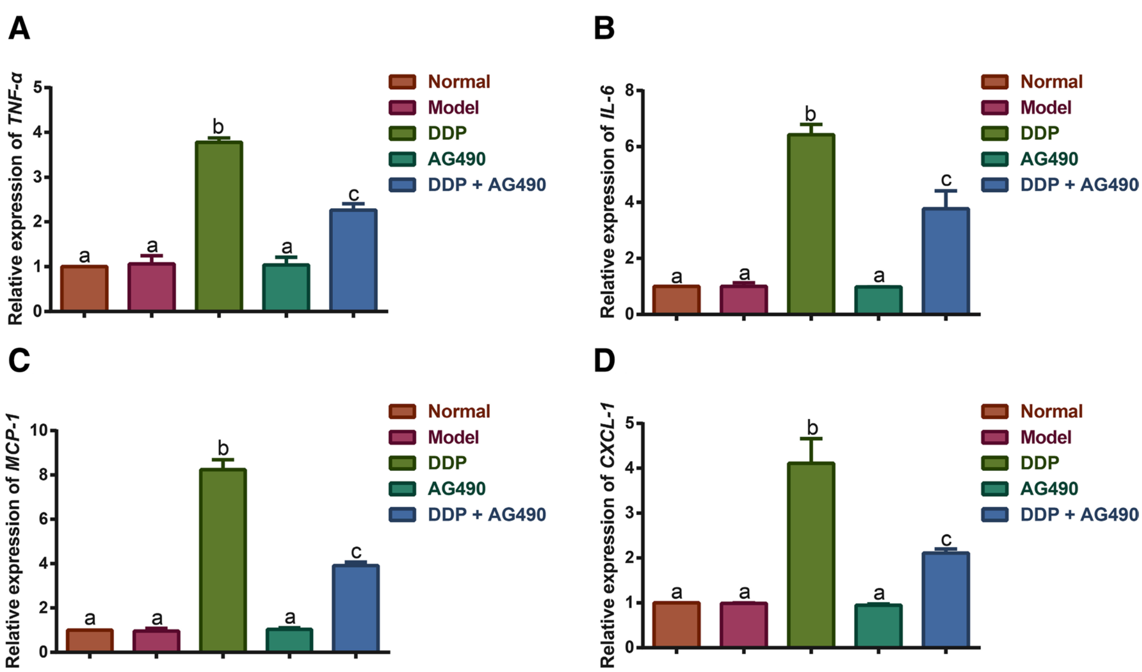

Fig. 5 Inhibitory effect of AG490 on DDP-induced inflammation in lung cancer mice ($n=10$). **a** TNF-α, **b** IL-6, **c** MCP-1, **d** CXCL-1; the same letter shows no statistical significance, i.e., $P>0.05$, while the different letter demonstrates the significant difference, i.e., $P<0.05$

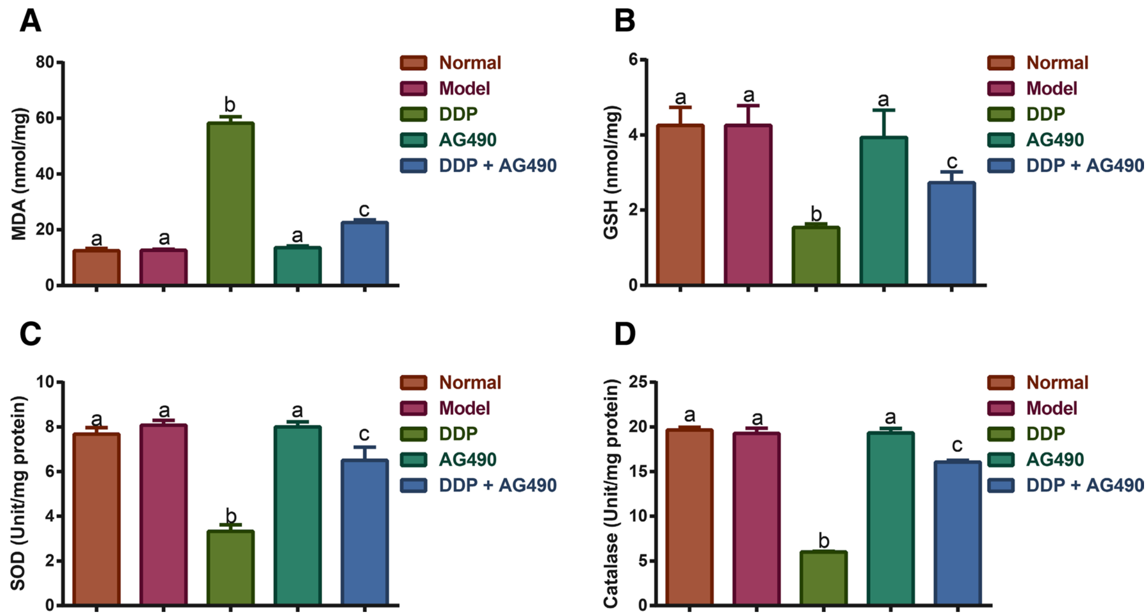

Fig. 6 Inhibitory effect of AG490 on DDP-induced oxidative stress in lung cancer mice ($n=10$). **a** MDA, **b** GSH, **c** SOD, **d** CAT; the same letter shows no statistical significance, i.e., $P>0.05$, while the different letter demonstrates the significant difference, i.e., $P<0.05$

Western blot assay in the AG490 group had no significant differences from the Normal group and the Model group (all $P>0.05$). Mice in the DDP group had higher expressions of anti-apoptotic proteins (Bax, cleaved caspase-9 and cleaved caspase-3) and lower Bcl-2 than those in the Normal group (all $P<0.05$). Moreover, mice in the DDP + AG490 group exhibited the recovered indicators of the above in varying degrees (all $P<0.05$, Fig. 7b, c). Furthermore, caspase-3 expression was also detected by immunohistochemistry staining, which was similar to the result of Western blot (Fig. 7d).

Discussion

Currently, intervention of the signaling pathway has become a trend in the field of cancer biotherapy, including lung cancer [25, 26]. Since JAK2/STAT3 signaling pathway is credited as the critical regulator of tumorigenesis to promote tumor cell proliferation, infiltration and metastasis and to participate in the immune escape mechanism of tumor, thus, suppressing this pathway may be helpful in inhibition of tumor cell growth and metastasis, as well as promotion of apoptosis [27, 28]. AG490, as one of the synthetic PTK inhibitors (tyrphostins) with anti-JAK2 activity, has been widely used to specifically block the JAK2/STAT3 signaling pathway by decreasing the mRNA and phosphorylation expression of JAK2 and STAT3 without affecting their total expressions [29, 30], being consistent with the results of our experiments. We hypothesized that the transcription activation might be regulated by the interaction between JAK2/STAT3 and other regulatory factors owing to phosphorylation. However, the reason for no changed total expressions of JAK2 and STAT3 is unclear because significant decreased in p-JAK2 and p-STAT3 were observed, which should be further explored in the future. It has been shown that AG490 can suppress TGF-β-induced migration and invasion of lung cancer cells [31], which could also curb lung cancer cell proliferation via reducing cyclin D1 in the paper of Kamran et al. [32]. Moreover, Ogata et al. demonstrated that AG490-induced inhibition of JAK/STAT could obviously suppress the tumor growth of lung cancer in human beings [33]. After administration of AG490 in our experiment, we found that inhibition of JAK2/STAT3 pathway could reduce the volume and mass of tumor, exhibiting the potential in molecular treatment of lung cancer. Moreover, the mRNA expressions of JAK and STAT3 and the protein expression of p-JAK and p-STAT3 were all increased in kidney tissues after the treatment with DDP, which was reversed by the AG490, indicating the AG490 could suppress DDP-induced activation of JAK2/STAT3 signaling pathway. Besides, we also noted that AG490 could enhance the sensitivity of lung cancer cells to DDP, and the combination of AG490 and DDP manifests the potent synergistic anti-tumor effect. However, although DDP is frequently used in clinical practice, the long-term massive administration could not only act on tumors, but also cause kidney damage, thereby affecting the life quality of patients [34, 35]. Additionally, AG490 in our study decreased DDP-induced increases in BUN and SCr and mitigate the kidney

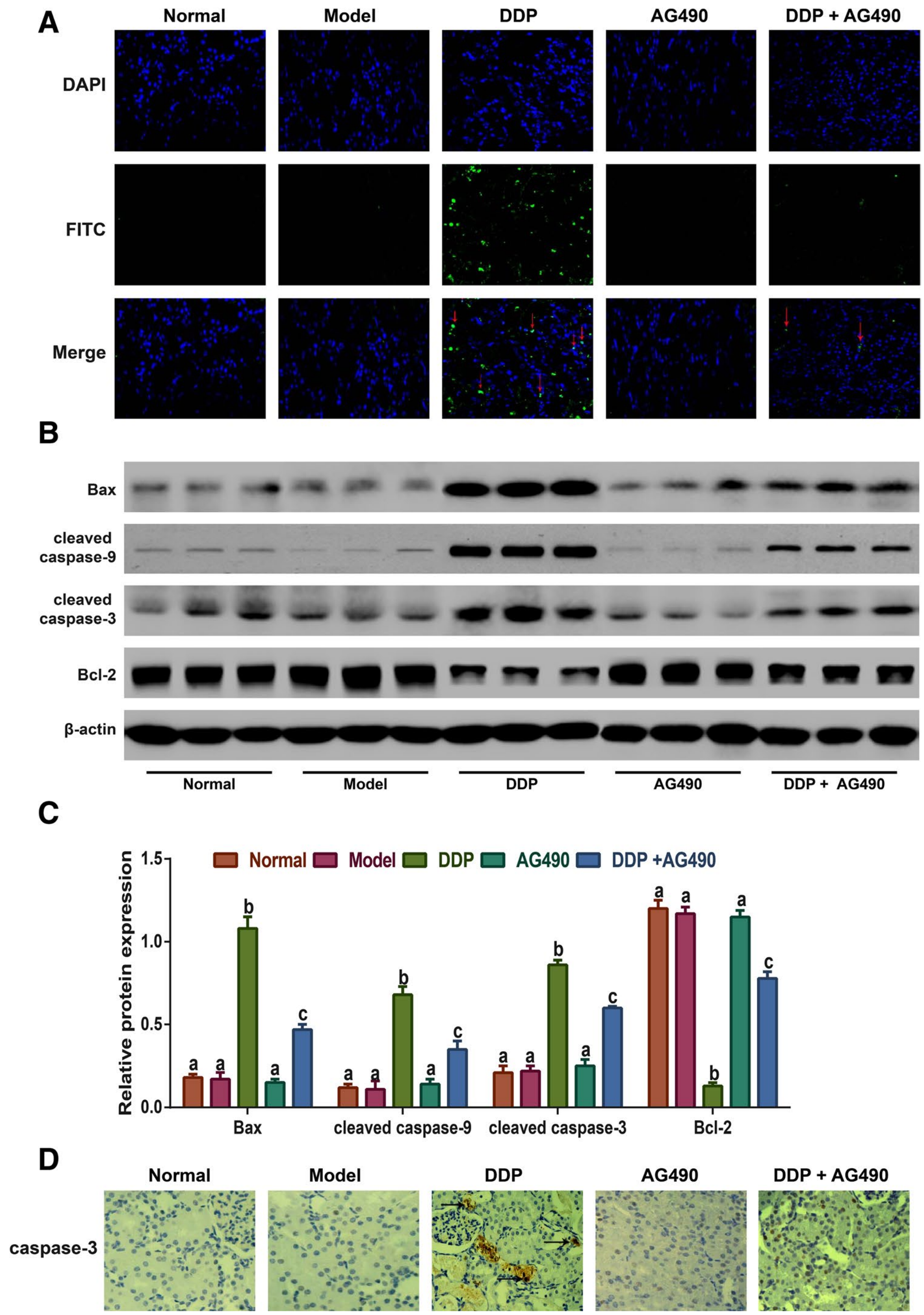

Fig. 7 Inhibitory effect of AG490 on DDP-induced kidney apoptosis in lung cancer mice ($n = 10$). **a** The kidney apoptosis of lung cancer mice detected by TUNEL method; **b**, **c** the expressions of apoptotic factors (including Bcl-2, Bax, cleaved caspase-9 and cleaved caspase-3) determined by western blot assay; The same letter shows no statistical significance, i.e., $P > 0.05$, while the different letter demonstrates the significant difference, i.e., $P < 0.05$

histological conditions as performed by HE staining, PAS staining and CD45 IHC staining. Thus, the combined use of AG490 and DDP could be a new way for lung cancer treatment.

Besides, DDP-induced kidney toxicity was so complicated that may be related to oxidative damage and inflammatory responses, resulting in upregulated MDA and decreases in GSH, SOD and CAT [36–38]. DDP and its metabolites can bind to GSH to form complex, contributing to the dysfunction of kidney tubular epithelial cells and kidney damage [39]. MDA could reflex the changes in the peroxidation of lipid and SOD plays a pivotal role in balancing the oxidation and anti-oxidation to prevent the cell damage [40, 41]. Importantly, emerging evidence has indicated the involvement of JAK2/STAT3 pathway in oxidative stress-induced damage [42]. In various cell types, inhibition of the JAK2/STAT3 signals could mitigate the oxidative damage induced by H_2O_2 [43, 44]. Furthermore, the inhibitory effect of AG490 on JAK2 could protect endothelial and tubular cells from oxidative stress-induced death [45], which might be a potential way to balance the oxidative stress after kidney damage. Additionally, existing studies have shown that in the DDP-induced kidney damage models of mouse, inflammatory cytokines (like TNF-α, IL-6, MCP-1 and CXCL-1) were abnormally increased, which would be decreased through inhibition of JAK2/STAT1/STAT3-SOCS3 signaling pathway [46, 47]. This signaling pathway, as a classical pathway, has been revealed to regulate the inflammatory responses in kidney ischemia or reperfusion damage [48]. Indeed, MDA was elevated with decreased GSH, SOD and CAT, as well as down-regulations of the above inflammatory cytokines in our models induced by DDP, which, however, was reversed partially by administration of AG490, suggesting that inhibition of JAK2/STAT3 pathway may alleviate oxidative stress and inflammatory responses in kidney tissues to minimize the DDP-induced acute kidney damage.

In recent years, people have paid much more attention to the kidney toxicity of DDP in the kidney cell apoptosis [46]. Research supported the notion that in the DDP-induced mitochondrial apoptosis, signal transduction was modulated by Bcl-2 family, including pro-apoptotic gene (Bax) and the anti-apoptotic gene (Bcl-2) [49]. Under the stimuli of DDP, Bax was activated, resulting in cytochrome C release from mitochondria to further activate the caspase-9/caspase-3, and finally triggered cell apoptosis [50]. In agreement with our study, inhibiting the activation of JAK2/STAT3 pathway could block cell apoptosis, which could protect the kidney tissues from the ischemia/reperfusion injury [51]. Ping et al. also discovered that AG490 could block the JAK2/STAT3 pathway to prevent the up-regulation of Bax/Bcl-2 ratio caused by HBx and to reduce the apoptosis of human kidney proximal tubule epithelial cells [52]. Notably, our mice with the combined use of DDP and AG490 had better recovery in these apoptotic factors caused by the single administration of DDP, and significant reductions in cell apoptosis, indicating that AG490 can improve the apoptosis in kidney tissues and the DDP-caused kidney damage.

Collectively, the inhibition of JAK2/STAT3 signaling pathway by AG490 could improve the oxidative stress, inflammation and kidney apoptosis to minimize DDP-induced AKI and curb the tumor growth in mice with lung cancer.

Acknowledgements The study was supported by Cangzhou Science and Technology R&D Instruction Project (no. 183302086).

Compliance with ethical standards

Conflict of interest The authors declare that they have no conflict of interest.

References

1. Chen YM. Update of epidermal growth factor receptor-tyrosine kinase inhibitors in non-small-cell lung cancer. J Chin Med Assoc. 2013;76:249–57.
2. Bareschino MA, Schettino C, Rossi A, Maione P, Sacco PC, Zeppa R, et al. Treatment of advanced non small cell lung cancer. J Thorac Dis. 2011;3:122–33.
3. Kates M, Perez X, Gribetz J, Swanson SJ, McGinn T, Wisnivesky JP. Validation of a model to predict perioperative mortality from lung cancer resection in the elderly. Am J Respir Crit Care Med. 2009;179:390–5.
4. Yiu KC, Juergens RA, Swaminath A. Multidisciplinary influence on care of lung cancer patients at the time of diagnosis: a patient survey. Clin Oncol (R Coll Radiol). 2016;28:667.
5. Wu YL, Zhou C, Hu CP, Feng J, Lu S, Huang Y, et al. Afatinib versus cisplatin plus gemcitabine for first-line treatment of Asian patients with advanced non-small-cell lung cancer harbouring EGFR mutations (LUX-Lung 6): an open-label, randomised phase 3 trial. Lancet Oncol. 2014;15:213–22.
6. Suntharalingam K, Mendoza O, Duarte AA, Mann DJ, Vilar R. A platinum complex that binds non-covalently to DNA and induces cell death via a different mechanism than cisplatin. Metallomics. 2013;5:514–23.
7. Barabas K, Milner R, Lurie D, Adin C. Cisplatin: a review of toxicities and therapeutic applications. Vet Comp Oncol. 2008;6:1–18.
8. Soni H, Matthews AT, Pallikkuth S, Gangaraju R, Adebiyi A. gamma-secretase inhibitor DAPT mitigates cisplatin-induced acute kidney injury by suppressing Notch1 signaling. J Cell Mol Med. 2019;23:260–70.
9. Zhou J, Fan Y, Zhong J, Huang Z, Huang T, Lin S, et al. TAK1 mediates excessive autophagy via p38 and ERK in cisplatin-induced acute kidney injury. J Cell Mol Med. 2018;22:2908–21.
10. Zundler S, Neurath MF. Integrating immunologic signaling networks: the JAK/STAT pathway in colitis and colitis-associated cancer. Vaccines (Basel). 2016;4:1–20.
11. Mullen M, Gonzalez-Perez RR. Leptin-induced JAK/STAT signaling and cancer growth. Vaccines (Basel). 2016;4:1–17.
12. Qing Y, Stark GR. Alternative activation of STAT1 and STAT3 in response to interferon-gamma. J Biol Chem. 2004;279:41679–85.
13. Li R, Rezk A, Miyazaki Y, Hilgenberg E, Touil H, Shen P, et al. Proinflammatory GM-CSF-producing B cells in multiple sclerosis and B cell depletion therapy. Sci Transl Med. 2015;7:310ra166.
14. Qin JZ, Zhang CL, Kamarashev J, Dummer R, Burg G, Dobbeling U. Interleukin-7 and interleukin-15 regulate the expression of the bcl-2 and c-myb genes in cutaneous T-cell lymphoma cells. Blood. 2001;98:2778–83.
15. Sarkar M, Khare V, Ghosh MK. The DEAD box protein p68: a novel coactivator of Stat3 in mediating oncogenesis. Oncogene. 2017;36:3080–93.
16. Levy DE, Inghirami G. STAT3: a multifaceted oncogene. Proc Natl Acad Sci USA. 2006;103:10151–2.
17. Li H, Lu Y, Pang Y, Li M, Cheng X, Chen J. Propofol enhances the cisplatin-induced apoptosis on cervical cancer cells via EGFR/JAK2/STAT3 pathway. Biomed Pharmacother. 2017;86:324–33.
18. Hu X, Ma J, Vikash V, Li J, Wu D, Liu Y, et al. Thymoquinone augments cisplatin-induced apoptosis on esophageal carcinoma through mitigating the activation of JAK2/STAT3 pathway. Dig Dis Sci. 2018;63:126–34.
19. Wang M, Lin T, Wang Y, Gao S, Yang Z, Hong X, et al. CXCL12 suppresses cisplatin-induced apoptosis through activation of JAK2/STAT3 signaling in human non-small-cell lung cancer cells. OncoTargets Ther. 2017;10:3215–24.

20. Zhu S, Zhang C, Weng Q, Ye B. Curcumin protects against acute renal injury by suppressing JAK2/STAT3 pathway in severe acute pancreatitis in rats. Exp Ther Med. 2017;14:1669–74.
21. Yang N, Luo M, Li R, Huang Y, Zhang R, Wu Q, et al. Blockage of JAK/STAT signalling attenuates renal ischaemia-reperfusion injury in rat. Nephrol Dial Transplant. 2008;23:91–100.
22. Orlans FB. Ethical decision making about animal experiments. Ethics Behav. 1997;7:163–71.
23. Hu R, Ma S, Ke X, Jiang H, Wei D, Wang W. Effect of interleukin-2 treatment combined with magnetic fluid hyperthermia on Lewis lung cancer-bearing mice. Biomed Rep. 2016;4:59–62.
24. Johansson LH, Borg LA. A spectrophotometric method for determination of catalase activity in small tissue samples. Anal Biochem. 1988;174:331–6.
25. Zheng H, Liu JF. Studies on the relationship between P13K/AKT signal pathway-mediated MMP-9 gene and lung cancer. Eur Rev Med Pharmacol Sci. 2017;21:753–9.
26. Song SG, Yu HY, Ma YW, Zhang F, Xu XY. Inhibition on Numb/Notch signal pathway enhances radiosensitivity of lung cancer cell line H358. Tumour Biol. 2016;37:13705–19.
27. Zhang ZR, Gao MX, Yang K. Cucurbitacin B inhibits cell proliferation and induces apoptosis in human osteosarcoma cells via modulation of the JAK2/STAT3 and MAPK pathways. Exp Ther Med. 2017;14:805–12.
28. Byun HJ, Darvin P, Kang DY, Sp N, Joung YH, Park JH, et al. Silibinin downregulates MMP2 expression via Jak2/STAT3 pathway and inhibits the migration and invasive potential in MDA-MB-231 cells. Oncol Rep. 2017;37:3270–8.
29. Zhou K, Chen J, Wu J, Wu Q, Jia C, Xu YXZ, et al. Atractylenolide III ameliorates cerebral ischemic injury and neuroinflammation associated with inhibiting JAK2/STAT3/Drp1-dependent mitochondrial fission in microglia. Phytomedicine. 2019;59:152922.
30. Zhao XB, Qin Y, Niu YL, Yang J. Matrine inhibits hypoxia/reoxygenation-induced apoptosis of cardiac microvascular endothelial cells in rats via the JAK2/STAT3 signaling pathway. Biomed Pharmacother. 2018;106:117–24.
31. Liu RY, Zeng Y, Lei Z, Wang L, Yang H, Liu Z, et al. JAK/STAT3 signaling is required for TGF-beta-induced epithelial-mesenchymal transition in lung cancer cells. Int J Oncol. 2014;44:1643–51.
32. Kamran MZ, Patil P, Shirsath K, Gude RP. Tyrosine kinase inhibitor AG490 inhibits the proliferation and migration and disrupts actin organization of cancer cells. J Environ Pathol Toxicol Oncol. 2013;32:361–71.
33. Ogata Y, Osaki T, Naka T, Iwahori K, Furukawa M, Nagatomo I, et al. Overexpression of PIAS3 suppresses cell growth and restores the drug sensitivity of human lung cancer cells in association with PI3-K/Akt inactivation. Neoplasia. 2006;8:817–25.
34. Zahedi K, Barone S, Destefano-Shields C, Brooks M, Murray-Stewart T, Dunworth M, et al. Activation of endoplasmic reticulum stress response by enhanced polyamine catabolism is important in the mediation of cisplatin-induced acute kidney injury. PLoS One. 2017;12:e0184570.
35. Veceric-Haler Z, Cerar A, Perse M. (Mesenchymal) Stem cell-based therapy in cisplatin-induced acute kidney injury animal model: risk of immunogenicity and tumorigenicity. Stem Cells Int. 2017;2017:7304643.
36. Wang Z, Li YF, Han XY, Sun YS, Zhang LX, Liu W, et al. Kidney protection effect of ginsenoside Re and its underlying mechanisms on cisplatin-induced kidney injury. Cell Physiol Biochem. 2018;48:2219–29.
37. Yan W, Xu Y, Yuan Y, Tian L, Wang Q, Xie Y, et al. Renoprotective mechanisms of Astragaloside IV in cisplatin-induced acute kidney injury. Free Radic Res. 2017;51:669–83.
38. Palipoch S, Punsawad C. Biochemical and histological study of rat liver and kidney injury induced by cisplatin. J Toxicol Pathol. 2013;26:293–9.
39. Ryoo IG, Shin DH, Kang KS, Kwak MK. Involvement of Nrf2-GSH signaling in TGFbeta1-stimulated epithelial-to-mesenchymal transition changes in rat renal tubular cells. Arch Pharm Res. 2015;38:272–81.
40. Seifi B, Kadkhodaee M, Delavari F, Mikaeili S, Shams S, Ostad SN. Pretreatment with pentoxifylline and *N*-acetylcysteine in liver ischemia reperfusion-induced renal injury. Ren Fail. 2012;34:610–5.
41. Son D, Kojima I, Inagi R, Matsumoto M, Fujita T, Nangaku M. Chronic hypoxia aggravates renal injury via suppression of Cu/Zn-SOD: a proteomic analysis. Am J Physiol Ren Physiol. 2008;294:F62–72.
42. Duan W, Yang Y, Yi W, Yan J, Liang Z, Wang N, et al. New role of JAK2/STAT3 signaling in endothelial cell oxidative stress injury and protective effect of melatonin. PLoS One. 2013;8:e57941.
43. Gorina R, Sanfeliu C, Galito A, Messeguer A, Planas AM. Exposure of glia to pro-oxidant agents revealed selective Stat1 activation by H_2O_2 and Jak2-independent antioxidant features of the Jak2 inhibitor AG490. Glia. 2007;55:1313–24.
44. Arany I, Megyesi JK, Nelkin BD, Safirstein RL. STAT3 attenuates EGFR-mediated ERK activation and cell survival during oxidant stress in mouse proximal tubular cells. Kidney Int. 2006;70:669–74.
45. Neria F, Castilla MA, Sanchez RF, Gonzalez Pacheco FR, Deudero JJ, Calabia O, et al. Inhibition of JAK2 protects renal endothelial and epithelial cells from oxidative stress and cyclosporin A toxicity. Kidney Int. 2009;75:227–34.
46. Malik S, Bhatia J, Suchal K, Gamad N, Dinda AK, Gupta YK, et al. Nobiletin ameliorates cisplatin-induced acute kidney injury due to its anti-oxidant, anti-inflammatory and anti-apoptotic effects. Exp Toxicol Pathol. 2015;67:427–33.
47. Sun M, Bu W, Li Y, Zhu J, Zhao J, Zhang P, et al. Danzhi Jiangtang Capsule ameliorates kidney injury via inhibition of the JAK-STAT signaling pathway and increased antioxidant capacity in STZ-induced diabetic nephropathy rats. Biosci Trends. 2019;12:595–604.
48. Si YN, Bao HG, Xu L, Wang XL, Shen Y, Wang JS, et al. Dexmedetomidine protects against ischemia/reperfusion injury in rat kidney. Eur Rev Med Pharmacol Sci. 2014;18:1843–51.
49. Park MS, De Leon M, Devarajan P. Cisplatin induces apoptosis in LLC-PK1 cells via activation of mitochondrial pathways. J Am Soc Nephrol. 2002;13:858–65.
50. Jiang M, Wang CY, Huang S, Yang T, Dong Z. Cisplatin-induced apoptosis in p53-deficient renal cells via the intrinsic mitochondrial pathway. Am J Physiol Ren Physiol. 2009;296:F983–93.
51. Lv J, Wang X, Liu SY, Liang PF, Feng M, Zhang LL, et al. Protective effect of Fenofibrate in renal ischemia reperfusion injury: involved in suppressing kinase 2 (JAK2)/transcription 3 (STAT3)/p53 signaling activation. Pathol Biol. 2015;63:236–42.
52. He P, Zhang D, Li H, Yang X, Li D, Zhai Y, et al. Hepatitis B virus X protein modulates apoptosis in human renal proximal tubular epithelial cells by activating the JAK2/STAT3 signaling pathway. Int J Mol Med. 2013;31:1017–29.